Appl. Phys. A (2016) 122:829
DOI 10.1007/s00339-016-0324-0

Applied Physics A
Materials Science & Processing

Free vibration of symmetric and sigmoid functionally graded nanobeams

M. A. Hamed[1] · M. A. Eltaher[1,2] · A. M. Sadoun[1,2] · K. H. Almitani[1]

Received: 16 April 2016 / Accepted: 28 July 2016 / Published online: 17 August 2016
© Springer-Verlag Berlin Heidelberg 2016

Abstract The objective of this paper was the investigation of vibration characteristics of both nonlinear symmetric power and sigmoid functionally graded nonlocal nanobeams. The volume fractions of metal and ceramic are assumed to be distributed through a beam thickness by sigmoid law distribution and symmetric power function. Structures with symmetric distribution with mid-plane such as ceramic–metal–ceramic and metal–ceramic–metal are proposed. Nonlocal differential Eringen's elasticity is exploited to incorporate size dependency of nanobeam. The kinematic relations of Euler–Bernoulli beam are proposed, with the assumption of a small strain. A nonlocal equation of motion of nanobeam is derived by using principle of virtual work and then discretized by finite element method to obtain numerical solution. Numerical results show the effects of the function distribution, gradient index and nonlocal parameter on natural frequencies of macro- and nanobeam. This model is helpful in the mechanical design of nanoelectromechanical systems manufactured from FGM.

1 Introduction

Recently, nanotechnology is concerned with fabrication of functionally graded materials (FGMs) and engineering structures at a nanoscale, which enables new generation of materials and devices with innovative properties [21]. FGMs are suitable for large structures (i.e., aircraft, space vehicles, automotive industries, optics, barrier coating, nuclear reactors and propulsion systems) and nanostructures (i.e., nanoelectromechanical systems, thin films, shape memory alloys and atomic force microscopes). A FGM is depicted by a continuous graduation of material composition in one or more dimensions from one material to another that provides an elegant solution to the problem of *high transverse shear stresses, interface cracking, delamination* and *residual stresses*. Power-law distribution (P-FGM) [3, 21–23, 39, 53, 54, 60] and exponential distribution (E-FGM) [4, 33, 43, 44] are frequently used to depict the variations of material properties distribution of FGMs.

It is observed that the stress concentrations appear in the interface layer when the material is continuously changing rapidly for both power and exponential functions distribution [9]. Therefore, Chi and Chung [15] suggested a sigmoid function, a combination of two types of P-FGM functions, to reduce the stress intensity factors in cracked structure. In addition, structures, which have ceramic constituent at top and bottom surfaces and have metallic core, can sustain a higher temperature more than power and exponential FGM.

By using powder metallurgy and thermal spraying techniques, Kapuria et al. [38] fabricated multilayered FG beam and then experimentally validated the results on static and free vibration. For sigmoid function, Ben-Oumrane et al. [9] analyzed theoretically a flexional bending of Al/Al_2O_3 S-FGM thick beams according to different beam theories. Mahi et al. [45] presented exact solutions to study the free vibration of a unified higher-order shear deformation theory. Material properties are proposed to be temperature dependent and vary continuously through the

✉ M. A. Hamed
mhamed@kau.edu.sa

[1] Mechanical Engineering Department, Faculty of Engineering, King Abdulaziz University, P.O. Box 80204, Jeddah 21589, Saudi Arabia

[2] Mechanical Design and Production Department, Faculty of Engineering, Zagazig University, Zagazig, Egypt

thickness according to E-FGM and S-FGM. Fereidoon and Mohyeddin [32] exploited differential quadrature method to analyze bending of thin functionally graded plates. Duc and Cong [17] investigated the nonlinear dynamic response of imperfect symmetric thin sigmoid functionally graded material (S-FGM) subjected to mechanical loads. Lee and Kim [41] studied thermal post-buckling and snap-through instabilities of P-FGM, E-FGM and S-FGM panels in hypersonic flows. Jung and Han [37] illustrated bending behavior of nonlocal S-FGM nanoplates with first-order shear deformation.

Tiny beam is the basic structure used in several applications such as nanoelectromechanical systems (NEMS), nanowires, nanoprobes, atomic force microscope (AFM), nanoactuators and nanosensors. For convincing designing of nanostructure, the size and length-scale effects and the atomic forces should be included in the mathematical formulation. The nonlocal elasticity theory developed by Eringen [29–31] is a promising theory which contains information about the forces between atoms and the internal length scale. The use of nonlocal continuum mechanics has found successful applications in several areas which include fracture mechanics, lattice dispersion of elastic waves, mechanics of dislocations and wave propagation in mechanics [52]. Reddy [51] developed analytical solutions for bending, buckling and vibration of isotropic beams using Euler–Bernoulli, Timoshenko, Reddy and Levinson beam theories.

A lot of researchers have motivated on FG of nanobeams using nonlocal Eringen's elasticity in differential model. According to power-law distribution of functionally graded nanobeams, Eltaher et al. [21, 22] presented a finite element model to study a static, buckling and dynamic behavior of Euler nanobeams. Eltaher et al. [23] illustrated the effect of neutral plane on natural frequencies and noted that the calculated frequency at mid-plane is overestimated than that at neutral axis. Tounsi et al. [59], Benguediab et al. [7] and Besseghier et al. [10] studied nonlocal chirality and thermal effects on buckling properties of double-walled carbon nanotubes (DWCNTs). Simsek and Yurtcu [55] examined analytically static bending and buckling of Timoshenko and Euler–Bernoulli nanobeams. Eltaher et al. [25, 26] adopted previous model to consider the shear effect by using Timoshenko nanobeams. Reddy et al. [53] developed a nonlinear finite element models for a static bending of FG nanobeams with moderate displacements and rotations. Uymaz [60], Rahmani and Pedram [50] used Navier's solution to study the free and forced vibration problem of a FG nanobeam. Kiani [39] proposed a mathematical model to explore vibrations and instabilities of moving FG nanobeams. The longitudinal and lateral equations of motion of the moving nanostructure were extracted by employing the nonlocal Rayleigh beam model.

Chaht et al. [14] presented bending and buckling behavior of FGM size-dependent nanobeams including the thickness stretching effect. Ebrahimi and Salari [18] used both Navier method and a semi-analytical differential transform method to investigate a free flexural vibrational of FG Euler nanobeams. Ebrahimi and Boreiry [19] investigated surface effects on nonlocal vibrational behavior of nanobeams. Salehipour et al. [54] presented a modified nonlocal elasticity theory for functionally graded materials by using an imaginary nonlocal strain tensor to directly obtain the nonlocal stress tensor. Rahmani and Jandaghian [49] developed an analytical solution of a buckling of third-order nanofunctionally graded beam by using Rayleigh–Ritz technique. Filiz and Aydogdu [33] studied a wave propagation in embedded functionally graded nanotubes conveying fluid. The material properties are changing exponentially in the thickness direction. Eltaher et al. [27] presented a review on nonlocal elastic models for bending, buckling, vibrations and wave propagation of nanoscale beams. Agwa and Eltaher [1] presented a vibration behavior of carbyne nanomechanical mass sensors with surface effect. Ebrahimi and Barati [20] investigated vibration behavior of magneto-electro-thermo-elastic functionally graded nanobeams based on a higher-order shear deformation beam theory. Hosseini and Rahmani [36] presented free vibration analysis of shallow and deep curved functionally graded (FG) nonlocal nanobeam. Sourki and Hoseini [56] investigated a vibration of a cracked microbeam based on the modified couple stress theory within the framework of Euler–Bernoulli beam theory. Eltaher et al. [28] presented nonlinear analysis of size-dependent and material-dependent nonlocal carbon nanotubes.

To satisfy the zero traction boundary conditions on the surfaces, Eltaher et al. [12] and Zidi et al. [62] studied thermo- and hygro-thermo-mechanical bending response of FG plates using refined shear deformation theory. Meziane et al. [47], Hebali et al. [35], Belabed et al. [5], Mahi and Tounsi [46] and Bennoun et al. [8] developed a simple and accurate shear deformation theory for bending and free vibration of FG plates without requiring any shear correction factor. Bourada et al. [13] presented a simple shear and normal deformations theory for FG beams. Hamidi et al. [34] presented an accurate sinusoidal plate theory for the thermomechanical bending analysis of FG sandwich plates. Yahia et al. [61] studied wave propagation in FG plates with porosities using various higher-order shear deformation plate theories. Bellifa et al. [6] and Ahouel et al. [2] investigated size-dependent mechanical behavior of FG trigonometric shear deformable nanobeams including neutral surface position concept. Bounouara et al. [11] proposed zeroth-order shear deformation theory to study vibration of FG plate with parabolic variation within the plate thickness and vanish on the plate surfaces.

From the literature review and to the best of the authors' knowledge, it can be concluded that no researchers have attempted to use a sigmoidal function and symmetric power distributions for FG nanobeams. In fact, all of the related studies use the power and exponential distribution for FG nanobeams. The present study is intended to fill this gap in the literature by considering a sigmoidal distribution through thickness of nanobeams. So, this paper presented a free vibration of a new FG nonlocal nanobeam. The manuscript is organized as follows. Section 2 describes the mathematical formulation and governing equations of sigmoidal FG nanobeams with Eringen's nonlocal elasticity and Euler–Bernoulli kinematics assumptions. Section 3 summarizes the displacement finite element model to study a buckling stability and free vibration of nanobeam. In Sect. 4, a code validation and numerical results are discussed. Section 5 summarizes concluding remarks.

2 Problem formulation

2.1 Spatial material graduation functions

Functionally graded materials (FGMs) are produced by combining various materials continuously though a specific spatial direction. The simplest and accepted homogenization methods to estimate the effective properties at micromechanics level are Voigt rule [48] and Mori–Tanaka mode [58]. The mechanical properties are graded across the thickness according to the Voigt model [42, 40].

The volume fraction of materials can be expressed as:

$$V_c = \left(\frac{1}{2}+\frac{z}{h}\right)^k \quad (0 \le k < \infty) \tag{1a}$$

$$V_c + V_m = 1 \tag{1b}$$

where V is the volume fraction, k is the nonnegative power exponent, and subscripts c and m represent the ceramic and metal, respectively. In the current analysis, symmetric power function (SP-FGM) and sigmoid function S-FGM are proposed.

The symmetric power function can be depicted by:

$$P_1(z) = (P_{surf} - P_{core})\left(\frac{-2z}{h}\right)^k + P_{core} \quad \left(\frac{-h}{2} \le z \le 0\right) \tag{2a}$$

$$P_2(z) = (P_{surf} - P_{core})\left(\frac{2z}{h}\right)^k + P_{core} \quad \left(0 \le z \le \frac{h}{2}\right) \tag{2b}$$

However, the sigmoid functional distribution can be described by:

$$P_1(z) = P_m V_m + P_C V_c = P_m + \frac{1}{2}(P_c - P_m)\left(1+\frac{2z}{h}\right)^k \quad \left(\frac{-h}{2} \le z \le 0\right) \tag{3a}$$

$$P_2(z) = P_m V_m + P_C V_c = P_c - \frac{1}{2}(P_c - P_m)\left(1-\frac{2z}{h}\right)^k \quad \left(0 \le z \le \frac{h}{2}\right) \tag{3b}$$

where P is material properties [Young's modulus (E), density (ρ) or Poisson's ratio (υ)] and subscripts surf, core, m and c are surface, core, metal and ceramics, respectively. The FG beam in the current manuscript is composed of aluminum metal [$E_m = 70$ GPa, $\rho_m = 2.7$ g/cm^3 and υ_m is 0.3] and ceramics of alumina [$E_c = 380$ GPa, $\rho_c = 3.96$ g/cm^3 and $\upsilon_c = 0.3$]. Delale and Erdogan [16] proved that the effect of Poisson's ratio on the deformation is much less than Young's modulus. So, the Poisson's ratio is assumed to be constant in this analysis. The distribution of Young's modulus and mass density through the beam thickness for ceramic–metal–ceramic (CMC), metal–ceramic–metal (MCM) and sigmoidal distribution is presented in Figs. 1, 2 and 3, respectively.

2.2 Geometrical fit conditions

Based on the Euler–Bernoulli theory, plane sections perpendicular to the axis of the beam before deformation remain plane, rigid and rotate such that they remain perpendicular to the (deformed) axis after deformation. The assumptions amount to neglecting the Poisson effect and transverse strains, Reddy (2014). The *displacement field* can be assumed as:

$$u(x,z) = u_0(x) - z\frac{dw_0(x)}{dx} \tag{4a}$$

$$w(x,z) = w_0(x) \tag{4b}$$

where u and w are the total displacements along the coordinate (x), and u_0 and w_0 denote the axial and transverse displacements of a point on the neutral axis. According to Euler hypothesis, the only *nonzero strain* is

$$\varepsilon_{xx}(x,z) = \frac{d}{dx}\left[u_0(x) - z\frac{dw_0(x)}{dx}\right] = \frac{du_0(x)}{dx} - z\frac{d^2w_0(x)}{dx^2} = \varepsilon^0_{xx} + z\varepsilon^1_{xx} \tag{5}$$

and *nonzero classical stress* can be presented by:

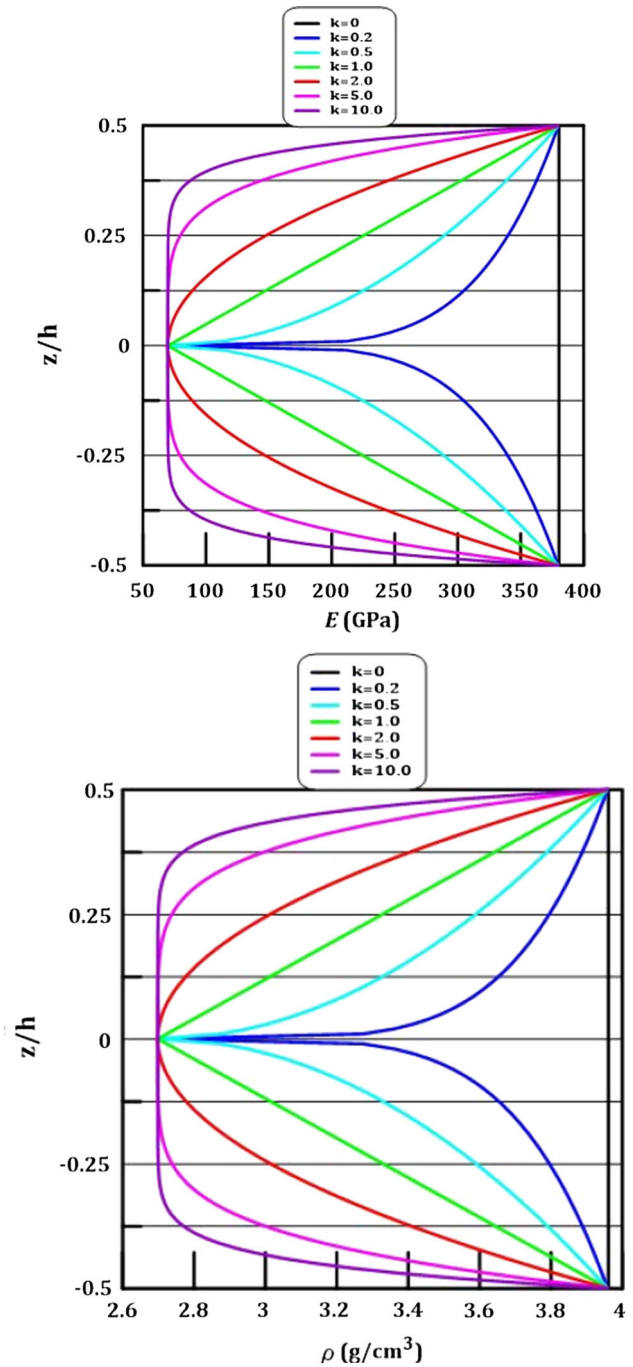

Fig. 1 Variation of Young's modulus and mass density through the beam thickness according to SP-FGM (CMC)

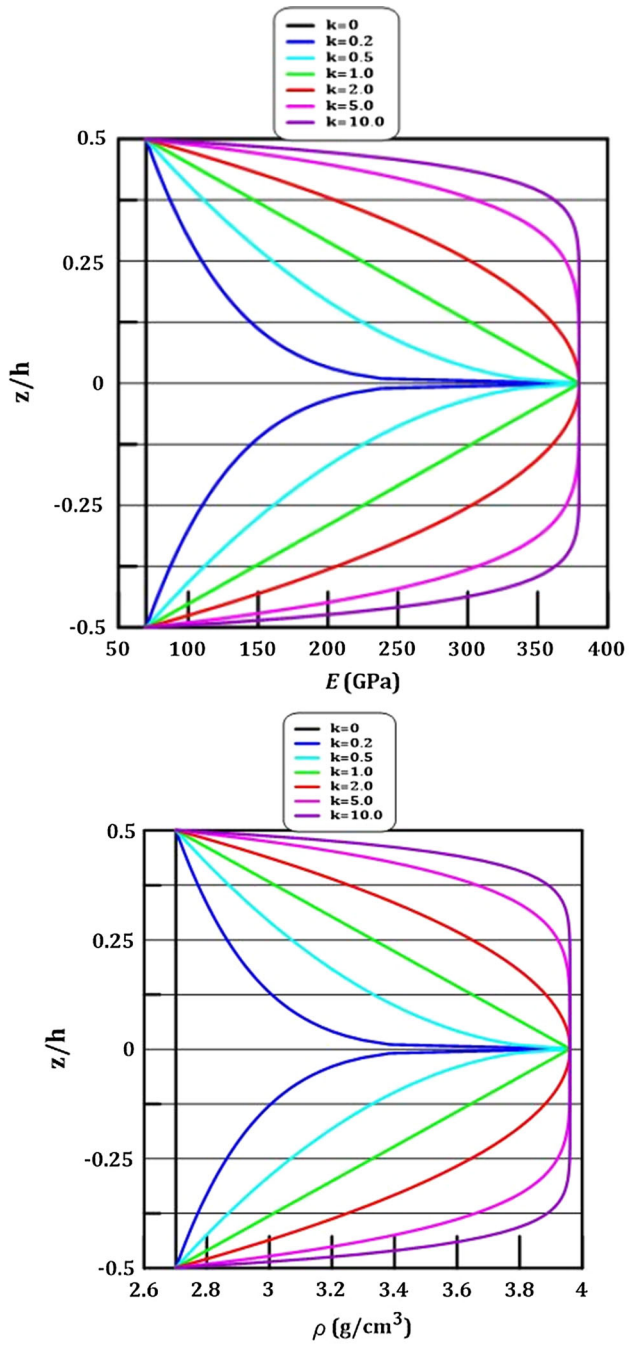

Fig. 2 Variation of Young's modulus and mass density through the beam thickness according to SP-FGM (MCM)

$$\sigma_{xx}(x,z) = E(z)\varepsilon_{xx}(x,z) = E(z)\left[\varepsilon^0_{xx} + z\varepsilon^1_{xx}\right] \tag{6}$$

Axial and bending moment can be written as:

$$N_{xx} = \int_A \sigma_{xx} dA = A_{11}\varepsilon^0_{xx} + B_{11}\varepsilon^1_{xx} \tag{7a}$$

$$M_{xx} = \int_A z\sigma_{xx} dA = B_{11}\varepsilon^0_{xx} + D_{11}\varepsilon^1_{xx} \tag{7b}$$

where

$$[A_{11}, B_{11}, D_{11}] = b\int_h E(z)\left[1, z, z^2\right]\mathrm{d}z$$

$$= b\left[\int_{-\frac{h}{2}}^{0} E_1(z)\left[1, z, z^2\right]\mathrm{d}z + \int_0^{\frac{h}{2}} E_2(z)\left[1, z, z^2\right]\mathrm{d}z\right] \tag{8}$$

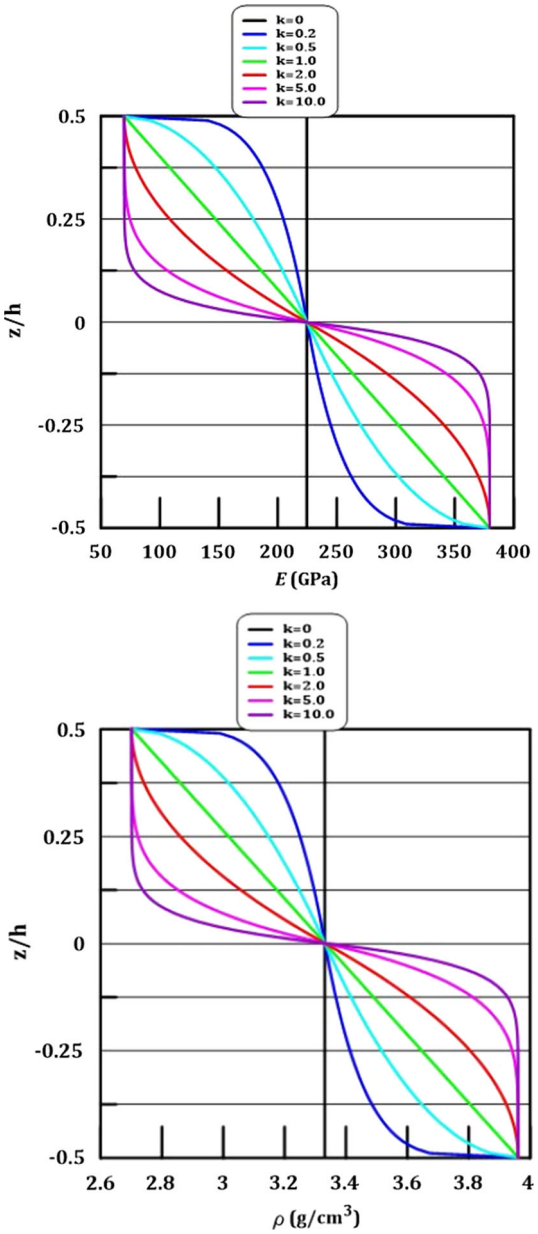

Fig. 3 Variation of Young's modulus and mass density through the beam thickness according to sigmoidal function

2.3 Nonlocal stress–strain relations

Based on the nonlocal differential Eringen elasticity theory, the nonlocal constitutive relation can be described by [31]:

$$\left(1-(e_0a)^2\nabla^2\right)\sigma_{ij}=t_{ij} \tag{9}$$

where ∇^2 is the Laplacian operator, t_{ij} is the classical macroscopic stress tensor, e_0 is a material constant, and a is the internal characteristic length. For Euler–Bernoulli nonlocal FG beam, Eq. (9) can be simplified as

$$\sigma_{xx}-\mu\frac{\partial^2\sigma_{xx}}{\partial x^2}=E(z)\varepsilon_{xx},\quad \left(\mu=e_0^2a^2\right) \tag{10}$$

and nonlocal axial and bending moment can be described by:

$$N-\mu\frac{\partial^2 N}{\partial x^2}=A_{11}\varepsilon_{xx}^0+B_{11}\varepsilon_{xx}^1 \tag{11a}$$

$$M-\mu\frac{\partial^2 M}{\partial x^2}=B_{11}\varepsilon_{xx}^0+D_{11}\varepsilon_{xx}^1 \tag{11b}$$

2.4 Nonlocal equations of motion

According to Hamilton's principle, the equation of motion of functionally graded beam can be derived to the following

$$\begin{aligned}&A_{11}\frac{\partial^2 u_0}{\partial x^2}+B_{11}\frac{\partial^3 w_o}{\partial x^3}+\left(1-\mu\frac{\partial^2}{\partial x^2}\right)f\\&\quad=I_0\frac{\partial^2 u_0}{\partial t^2}-I_1\frac{\partial^3 w_0}{\partial t^2\partial x}-\mu\left[I_0\frac{\partial^4 u_0}{\partial t^2\partial x^2}-I_1\frac{\partial^5 w_0}{\partial t^2\partial x^3}\right]\end{aligned} \tag{12a}$$

$$\begin{aligned}&B_{11}\left(\frac{\mathrm{d}^3u_0}{\mathrm{d}x^3}\right)+D_{11}\frac{\mathrm{d}^4w_0}{\mathrm{d}x^4}+\left(1-\mu\frac{\partial^2}{\partial x^2}\right)q\\&\quad+\left(1-\mu\frac{\partial^2}{\partial x^2}\right)\left(\bar{N}\frac{\partial^2 w_0}{\partial x^2}\right)\\&\quad=\left(1-\mu\frac{\partial^2}{\partial x^2}\right)\left[I_0\frac{\partial^2 w_0}{\partial t^2}+I_1\frac{\partial^3 u_0}{\partial t^2\partial x}-I_2\frac{\partial^4 w_0}{\partial t^2\partial x^2}\right]\end{aligned} \tag{12b}$$

where f is the axial distributed force in x-direction, q is the transverse distributed force in z-direction, and $\bar{N}$ is the axial compressive load normal to the cross section and applied at the neutral axis. Inertia terms I_0, I_1 and I_2 can be described by:

$$\begin{aligned}[I_0,I_1,I_2]&=b\int_h\rho(z)\left[1,z,z^2\right]\mathrm{d}z\\&=b\left[\int_{-\frac{h}{2}}^{0}\rho_1(z)\left[1,z,z^2\right]\mathrm{d}z+\int_0^{\frac{h}{2}}\rho_2(z)\left[1,z,z^2\right]\mathrm{d}z\right]\end{aligned} \tag{13}$$

3 Numerical formulation

The displacement components at the mid-plane (that is coincident with neutral plane in the current material distributions) of a beam element can be described as [24]:

- In-plane displacement u_0

$$u_0^{(e)}(x,t)=\sum_{i=1}^{2}N_iU_i(t)=N_1U_1(t)+N_2U_2(t)$$

where $i=1,2$ (14a)

- Transverse displacement w_o

$$w_0^{(e)}(x,t) = \sum_{k=1}^{4} \tilde{N}_k \tilde{W}_k = \tilde{N}_1 W_1 + \tilde{N}_2 \theta_1 + \tilde{N}_3 W_2 + \tilde{N}_4 \theta_2 \tag{14b}$$

where U, W and θ are the nodal displacements and slope, respectively. N_i is the Lagrangian interpolation function for in-plane displacement, and $\tilde{N}_k$ is the Hermitian interpolation shape function for transverse displacements. The variational statement of nonlocal Euler–Bernoulli beam has the following form [57]:

$$\begin{aligned}
&\int_0^T \int_0^L \Bigg\{ \Bigg(\left[-\int_{-\frac{h}{2}}^{0} E_1(z)\mathrm{d}z - \int_0^{\frac{h}{2}} E_2(z)\mathrm{d}z \right] \frac{\partial u_0}{\partial x}\frac{\partial \delta u_0}{\partial x} + \left[\int_{-\frac{h}{2}}^{0} zE_1(z)\mathrm{d}z - \int_0^{\frac{h}{2}} zE_2(z)\mathrm{d}z \right] \frac{\partial^2 w_0}{\partial x^2}\frac{\partial \delta u_0}{\partial x} \\
&+ \left[\int_{-\frac{h}{2}}^{0} zE_1(z)\mathrm{d}z + \int_0^{\frac{h}{2}} zE_2(z)\mathrm{d}z \right] \frac{\partial u_0}{\partial x}\frac{\partial^2 \delta w_0}{\partial x^2} + \left[-\int_{-\frac{h}{2}}^{0} z^2E_1(z)\mathrm{d}z - \int_0^{\frac{h}{2}} z^2E_2(z)\mathrm{d}z \right] \frac{\partial^2 w_0}{\partial x^2}\frac{\partial \delta w_0}{\partial x^2} \Bigg) \\
&+ \left(f\delta u_0 + \mu \frac{\partial f}{\partial x}\frac{\partial \delta u_0}{\partial x} \right) + \left(q\delta w_0 - \mu q \frac{\partial^2 \delta w_0}{\partial x^2} \right) + \left(\bar{N}\frac{\partial w_0}{\partial x}\frac{\partial \delta w_0}{\partial x} - \mu \bar{N}\frac{\partial^2 w_0}{\partial x^2}\frac{\partial^2 \delta w_0}{\partial x^2} \right) \\
&+ \left(I_0 \frac{\partial u_0}{\partial t}\frac{\partial \delta u_0}{\partial t} - \mu I_0 \frac{\partial^3 u_0}{\partial t^2 \partial x}\frac{\partial \delta u_0}{\partial x} \right) + \left(I_0 \frac{\partial w_0}{\partial t}\frac{\partial \delta w_0}{\partial t} + \mu I_0 \frac{\partial^2 w_0}{\partial t^2}\frac{\partial^2 \delta w_0}{\partial x^2} + I_2 \frac{\partial^2 w_0}{\partial t \partial x}\frac{\partial^2 \delta w_0}{\partial t \partial x} - \mu I_2 \frac{\partial^4 w_0}{\partial t^2 \partial x^2}\frac{\partial^2 \delta w_0}{\partial x^2} \right) \\
&+ \left(I_1 \frac{\partial^2 u_0}{\partial t \partial x}\frac{\partial \delta w_0}{\partial t} + \mu I_1 \frac{\partial^3 u_0}{\partial t^2 \partial x}\frac{\partial^2 \delta w_0}{\partial x^2} - I_1 \frac{\partial^2 w_0}{\partial t \partial x}\frac{\partial \delta u_0}{\partial t} + I_1 \mu \frac{\partial^4 w_0}{\partial t^2 \partial x^2}\frac{\partial \delta u_0}{\partial x} \right) \Bigg\} \mathrm{d}x\mathrm{d}t + \int_0^t \left[\bar{N}_B \delta u_0 + \bar{V}_B \delta w_0 + \bar{M}_B \frac{\partial \delta w_0}{\partial x} \right]_0^L \mathrm{d}t = 0
\end{aligned} \tag{15}$$

By substituting Eq. (14) into Eq. (15) and integrating over the domain, the following equation of motion is derived

$$(M_\mathrm{l} + \mu M_\mathrm{nl})\ddot{Y} + K_\mathrm{s} Y + K_\mathrm{G} Y = F + Q \tag{16}$$

where M_l and $M\mathrm{n_l}$ are local and nonlocal mass matrices, respectively. K_s is the stiffness matrix of FG beam, K_G is the geometrical stiffness matrix, Y is the generalized displacement vector, and F and Q are the distributed force vector and concentrated force vector, respectively. The element matrices and force vectors can be represented by:

- The mass matrices can be represented by

$$\begin{aligned}
M_\mathrm{l} &= \int_0^l I_0 N_i N_j \mathrm{d}x + \int_0^l \left(I_0 \tilde{N}_k \tilde{N}_1 + I_2 \frac{\partial \tilde{N}_k}{\partial x}\frac{\partial \tilde{N}_1}{\partial x} \right) \mathrm{d}x \\
&+ \int_0^l \left(I_1 \frac{\partial N_i}{\partial x}\tilde{N}_1 + I_1 \frac{\partial^2 \tilde{N}_1}{\partial x^2} N_i \right) \mathrm{d}x
\end{aligned} \tag{17a}$$

$$\begin{aligned}
M_\mathrm{nl} &= -\int_0^l I_0 \frac{\partial N_i}{\partial x}\frac{\partial N_j}{\partial x}\mathrm{d}x \\
&+ \int_0^l \left(I_0 \tilde{N}_k \frac{\partial^2 \tilde{N}_1}{\partial x^2} - I_2 \frac{\partial^2 \tilde{N}_k}{\partial x^2}\frac{\partial^2 \tilde{N}_1}{\partial x^2} \right) \mathrm{d}x \\
&+ \int_0^l \left(I_1 \frac{\partial N_i}{\partial x}\frac{\partial^2 \tilde{N}_1}{\partial x^2} + I_1 \frac{\partial^2 \tilde{N}_1}{\partial x^2}\frac{\partial N_i}{\partial x} \right) \mathrm{d}x
\end{aligned} \tag{17b}$$

- Element stiffness matrix can be calculated by

$$K_\mathrm{u} = \int_0^l \left[-\int_{-\frac{h}{2}}^{0} E_1(z)\mathrm{d}z - \int_0^{\frac{h}{2}} E_2(z)\mathrm{d}z \right] \frac{\partial N_i}{\partial x}\frac{\partial N_j}{\partial x}\mathrm{d}x \quad \text{where } i \text{ and } j = 1,2 \tag{17c}$$

$$K_\mathrm{w} = \int_0^l \left[-\int_{-\frac{h}{2}}^{0} z^2E_1(z)\mathrm{d}z - \int_0^{\frac{h}{2}} z^2E_2(z)\mathrm{d}z \right] \frac{\partial \tilde{N}_k}{\partial x}\frac{\partial \tilde{N}_1}{\partial x}\mathrm{d}x \quad \text{where } k \text{ and } l = 1,2,3,4 \tag{17d}$$

$$\begin{aligned}
K_\mathrm{uw} &= \int_0^l \left[\int_{-\frac{h}{2}}^{0} zE_1(z)\mathrm{d}z + \int_0^{\frac{h}{2}} zE_2(z)\mathrm{d}z \right] \frac{\partial^2 \tilde{N}_k}{\partial x^2}\frac{\partial N_i}{\partial x}\mathrm{d}x \\
&+ \int_0^l \left[\int_{-\frac{h}{2}}^{0} zE_1(z)\mathrm{d}z + \int_0^{\frac{h}{2}} zE_2(z)\mathrm{d}z \right] \frac{\partial N_i}{\partial x}\frac{\partial^2 \tilde{N}_k}{\partial x^2}\mathrm{d}x
\end{aligned} \tag{17e}$$

$$K_s = K_u + K_w + K_{uw} \tag{17f}$$

- Element geometrical stiffness matrix can be represented by

$$K_G = \int_0^L \left[-\bar{N} \frac{\partial \tilde{N}_k}{\partial x} \frac{\partial \tilde{N}_1}{\partial x} + \mu \bar{N} \frac{\partial^2 \tilde{N}_k}{\partial x^2} \frac{\partial^2 \tilde{N}_1}{\partial x^2} \right] dx \tag{17g}$$

- The force vector can be represented by

$$F = q \int_0^L \left[\tilde{N}_k - \mu \frac{\partial^2 \tilde{N}_k}{\partial x^2} \right] dx + \int_0^L \left[f N_i + \mu \frac{\partial f}{\partial x} \frac{\partial N_i}{\partial x} \right] dx \tag{17h}$$

4 Numerical results

Here numerical examples are considered. In all cases, the dimensions of beam geometry are described as Eltaher et al. [21]. These values are used only for the purpose of numerically evaluating the parametric effects of nonlocal parameter (μ), material distribution (k) and functional distribution (P). The beam was assumed to be simply supported at both ends: a mesh of 50 elements (with linear approximation of u and hermite cubic approximation of w).

Table 1 presents the first five nondimensional frequencies of S-FGM with varying nonlocal parameter (μ) and material distribution (k). Fixing material distribution parameter and varying the nonlocal parameter results in a significant change in the natural frequencies. During this study, it is also found, as others have, that for simply supported nanobeams, natural frequencies decrease as the nonlocal parameter increases. For a case in hand, as the nonlocal parameter changes from 0 to 4×10^{-12}, the first and fifth frequencies reduce by about 15.5 and 60 %, respectively, at a constant material distribution $k = 0.5$. This emphasizes the significance of the nonlocal effect on the natural frequency of beam. It is also noted that for a sigmoidal distribution, the natural frequencies decreased by increasing the material parameter distribution (k), as shown in Table 1. The first fundamental frequency is reduced by 5 % as k changing from 0 to 10. Qualitative behavior of

Table 1 Dimensionless frequencies for different material distribution and nonlocal parameters for S-FGM

$\mu \times 10^{-12}$	λ_i	$K = 0.0$	$K = 0.1$	$K = 0.2$	$K = 0.5$	$K = 1$	$K = 2$	$K = 5$	$K = 10$
0	λ_1	15.9993	15.9892	15.9669	15.8732	15.7215	15.5227	15.3202	15.2532
	λ_2	64.808	64.5754	64.0489	61.97	58.9333	55.465	52.3957	51.4629
	λ_3	149.0202	148.5186	147.3818	142.9129	136.4318	129.092	122.6488	120.6998
	λ_4	175.7171	175.574	175.2376	173.7431	171.0262	167.0211	162.5555	161.013
	λ_5	273.5657	272.6656	270.6361	262.8162	251.9366	240.3158	230.7582	227.9857
1	λ_1	15.3556	15.2437	15.2222	15.1329	14.9878	14.7978	14.6041	14.5398
	λ_2	54.4681	54.1646	53.7332	52.0279	49.5288	46.6634	44.1189	43.3442
	λ_3	104.7114	104.2463	103.4783	100.4493	96.0286	90.9861	86.5306	85.1778
	λ_4	156.5851	155.5122	153.5614	146.9413	138.4686	129.4637	121.7915	119.4957
	λ_5	167.6366	167.946	168.4722	169.3441	168.9673	166.9546	163.5984	160.6316
2	λ_1	14.656	14.5932	14.5727	14.487	14.348	14.1656	13.9792	13.9177
	λ_2	47.7991	47.5702	47.1961	45.7159	43.543	41.0469	38.8265	38.1496
	λ_3	85.2585	84.9094	84.2911	81.8502	78.2814	74.2022	70.5908	69.4931
	λ_4	121.0426	120.4581	119.3393	115.0039	108.852	102.0059	96.0627	94.2735
	λ_5	153.486	152.7949	151.4536	146.2149	138.7001	130.2858	122.9668	120.7634
3	λ_1	14.0643	14.0184	13.9986	13.9163	13.7825	13.6069	13.4274	13.3677
	λ_2	43.1101	42.9154	42.5805	41.2548	39.3067	37.0662	35.071	34.4624
	λ_3	73.7371	73.4441	72.9123	70.8119	67.7385	64.2221	61.1063	60.1588
	λ_4	102.2118	101.7451	100.8457	97.3285	92.268	86.5753	81.5986	80.0955
	λ_5	127.8521	127.287	126.1843	121.8705	115.6658	108.6996	102.6273	100.7972
4	λ_1	13.5452	13.5078	13.4888	13.4094	13.2804	13.1109	12.9375	12.8799
	λ_2	39.578	39.4048	39.0989	37.8876	36.1065	34.0563	32.2294	31.6719
	λ_3	65.9003	65.6426	65.1689	63.2973	60.5576	57.4213	54.6411	53.7953
	λ_4	90.0997	89.6981	88.9214	85.8749	81.4708	76.4949	72.131	70.8111
	λ_5	111.8704	111.3805	110.422	106.6692	101.2647	95.189	89.8873	88.2886

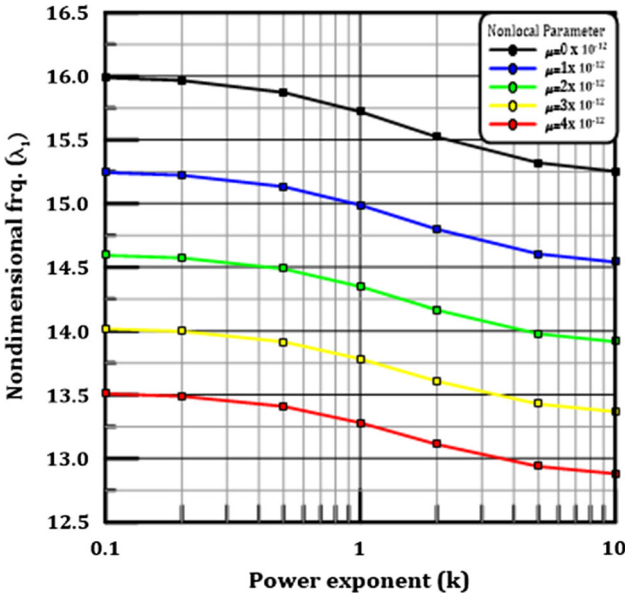

Fig. 4 Variation of the fundamental frequency for varying material distribution and nonlocal parameter of S-FGM

Table 1 for the first fundamental frequency λ_1 is illustrated in Fig. 4. From Fig. 4, it is observed that the fundamental frequency is reduced smoothly by changing the material distribution from 0 to 10 for a certain value of nonlocal parameter.

The effects of both size effect and material distribution on the first five fundamental frequencies of ceramics–metal–ceramics functionally graded nanobeam are presented in Table 2 and Fig. 5. As concluded form Table 2 and Fig. 5, the frequencies are assumed to be constant as the material distribution changes from 0 to 1; however, they are reduced significantly as the material parameter changes from 1 to 10. In addition, the nonlocal parameter tends to reduce the fundamental frequency of FG beam at a specific material distribution.

The variation of frequencies of metal–ceramics–metal functional graded nanobeams with a nonlocal parameter and material distribution is illustrated in Table 3. It is noted that the nonlocal parameter has the same effect on the natural frequencies for SP-FGM (MCM) as SP-FGM (CMC) and S-FGM. It is observed that the increase in

Table 2 Dimensionless frequencies for different material distribution and nonlocal parameters for SP-FGM (CMC)

$\mu \times 10^{-12}$	λ_i	$K = 0.0$	$K = 0.1$	$K = 0.2$	$K = 0.5$	$K = 1$	$K = 2$	$K = 5$	$K = 10$
0	λ_1	19.0664	19.0938	19.0899	18.9602	18.5579	17.6391	15.577	13.8059
	λ_2	77.2323	77.3618	77.3621	76.8671	75.2659	71.548	63.1723	55.9695
	λ_3	177.5904	177.9656	178.031	177.0266	173.4458	159.334	138.2242	126.2572
	λ_4	209.4059	204.4702	200.0261	188.9825	175.7171	164.9282	145.5623	128.8836
	λ_5	326.0145	326.9285	327.2349	325.7754	319.4982	303.9542	268.0914	237.135
1	λ_1	18.2997	18.3223	18.3162	18.1881	17.8002	16.9171	14.9413	13.2445
	λ_2	64.9103	65.004	64.9917	64.5517	63.1874	60.0571	53.037	47.0051
	λ_3	124.7869	124.9566	124.9255	124.0619	121.4254	115.4035	101.9221	90.3412
	λ_4	186.6059	186.8017	186.7074	180.292	167.6366	152.0069	131.8678	120.4512
	λ_5	199.7762	195.0675	190.8277	185.3177	181.3003	172.2721	152.1908	134.9586
2	λ_1	17.4648	17.488	17.4826	17.3615	16.9923	16.1489	14.2622	12.642
	λ_2	56.9628	57.0398	57.025	56.6303	55.4267	52.6774	46.5239	41.2376
	λ_3	101.6041	101.719	101.6742	100.9314	98.7548	93.8422	82.8971	73.5022
	λ_4	144.249	144.3521	144.2396	143.0845	139.9177	132.9201	117.4614	104.2114
	λ_5	182.9126	182.9452	182.7226	172.6997	160.5772	145.6058	126.3148	115.3789
3	λ_1	16.7612	16.7828	16.7783	16.6622	16.3084	15.4995	13.6878	12.1328
	λ_2	51.3751	51.4416	51.4258	51.065	49.9751	47.4945	41.9483	37.1856
	λ_3	87.8741	87.9632	87.9163	87.2569	85.3612	81.1086	71.6561	63.5458
	λ_4	121.8081	121.8777	121.7684	120.764	118.0678	112.1521	99.1215	87.9583
	λ_5	152.3642	152.3689	152.1651	150.7719	147.2963	139.8657	121.4089	109.8303
4	λ_1	16.1412	16.1628	16.1579	16.0466	15.7051	14.9262	13.1823	11.6842
	λ_2	47.1657	47.2248	47.2085	46.8741	45.871	43.5929	38.5039	34.1341
	λ_3	78.5347	78.609	78.5625	77.9641	76.263	72.4603	64.0196	56.7793
	λ_4	107.3738	107.4266	107.3233	106.4237	104.0364	98.8185	87.3433	77.5152
	λ_5	133.3184	133.3121	133.1252	131.8889	128.8348	122.3291	108.1758	96.077

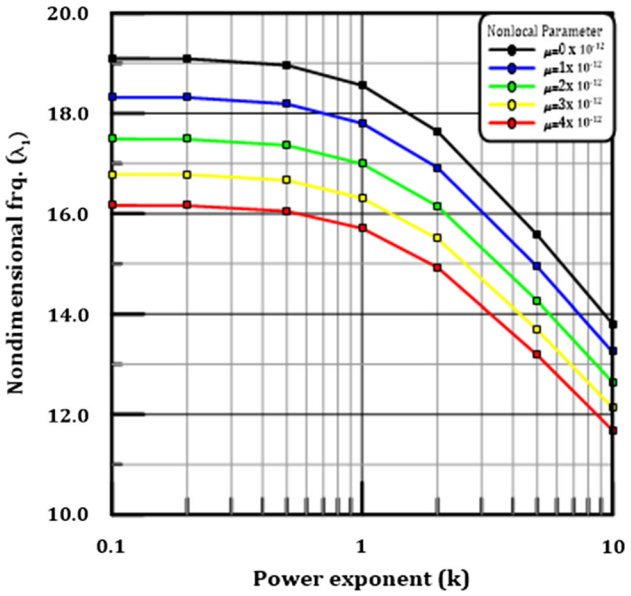

Fig. 5 Variation of the fundamental frequency for varying material distribution and nonlocal parameter of SP-FGM (CMC)

material distribution tends to increase the frequency at a constant nonlocal parameter. For example, at a zero nonlocal parameter, the first frequency increased from 9.9109 to 17.4289 as material distribution increased from 0 to 10. Graphical illustration of nonlocal parameter and material distribution effects on the fundamental frequency of MCM functionally graded nanobeam is shown in Fig. 6. From this figure, it can be concluded that the first frequency increased linearly with a material graduation and decreased with nonlocal parameter.

5 Conclusions

A numerical finite element model was developed to investigate the dynamic behavior of both nonlinear symmetric power and sigmoid functionally graded nonlocal nanobeams. The assumed material distributions are symmetrical with mid-plane. Nonlocal differential Eringen's elasticity is proposed to consider the size dependency of nanobeam.

Table 3 Dimensionless frequencies for different material distribution and nonlocal parameters for SP-FGM (MCM)

$\mu \times 10^{-12}$	λ_i	$K = 0.0$	$K = 0.1$	$K = 0.2$	$K = 0.5$	$K = 1$	$K = 2$	$K = 5$	$K = 10$
0	λ_1	9.9109	10.3759	10.785	11.7759	12.9489	14.4029	16.3185	17.4289
	λ_2	40.1444	42.0149	43.6602	47.6551	52.3882	58.2715	66.0421	70.5574
	λ_3	92.3086	96.5518	100.2896	109.3862	120.2024	133.7005	151.6157	162.0719
	λ_4	108.8459	126.2572	138.2242	159.334	175.7171	188.9825	200.0261	204.4702
	λ_5	169.457	177.0806	183.8124	200.2602	219.9257	244.6194	277.6399	297.041
1	λ_1	9.5112	9.9601	10.354	11.309	12.4367	13.8335	15.6701	16.7328
	λ_2	33.7392	35.3225	36.7139	40.0885	44.0795	49.0299	55.5514	59.3325
	λ_3	64.8621	67.9132	70.5939	77.0927	84.7739	94.2947	106.8261	114.0859
	λ_4	96.9947	101.6006	105.6434	115.4283	126.9656	141.2257	159.9292	170.7309
	λ_5	103.8405	120.4512	131.8678	151.6562	166.8904	180.292	190.8277	195.0675
2	λ_1	9.0779	9.5053	9.8806	10.7915	11.8666	13.1994	14.9528	15.9681
	λ_2	29.6082	31.0013	32.2252	35.1923	38.6988	43.0452	48.7651	52.0788
	λ_3	52.8122	55.3138	57.5102	62.8285	69.1032	76.8643	87.0532	92.9424
	λ_4	74.9783	78.5747	81.7282	89.3479	98.3089	109.351	123.779	132.0832
	λ_5	95.075	99.7086	103.7653	113.5415	124.9916	139.0319	157.265	167.7013
3	λ_1	8.7119	9.122	9.4822	10.3561	11.3877	12.6668	14.3493	15.3243
	λ_2	26.7039	27.9625	29.0682	31.7477	34.913	38.834	43.991	46.9765
	λ_3	45.6755	47.8467	49.7522	54.3635	59.7991	66.5154	75.3212	80.4049
	λ_4	63.3139	66.3638	69.037	75.4914	83.0737	92.4049	104.5773	111.573
	λ_5	79.1965	83.0731	86.4656	94.6354	104.1934	115.8978	131.0713	139.743
4	λ_1	8.3899	8.7849	9.132	9.9731	10.967	12.1987	13.8196	14.7577
	λ_2	24.5159	25.673	26.6891	29.1514	32.0589	35.6596	40.3928	43.1322
	λ_3	40.8211	42.7656	44.4718	48.5993	53.4619	59.4666	67.3331	71.8714
	λ_4	55.8111	58.506	60.8674	66.5669	73.2583	81.487	92.2117	98.3703
	λ_5	69.2968	72.6967	75.6713	82.8322	91.2049	101.4503	114.7204	122.298

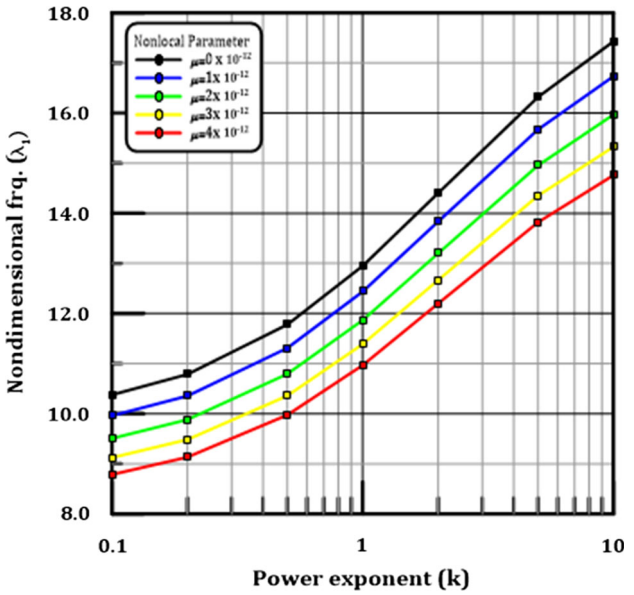

Fig. 6 Variation of the fundamental frequency for varying material distribution and nonlocal parameter of SP-FGM (MCM)

The most findings of this study may be summarized as:

- The nonlocal size parameter tends to decrease the frequencies of nanobeams.
- The material parameter k has different effects on the frequencies of nanobeams. By increasing k, the frequencies decrease in case of S-FGM distribution and increase in case of SP-FGM (MCM). However, in case of SP-FGM (CMC), the frequencies are constant in the range of $0 \leq k \leq 1$ and decreased in the range $1 \leq k \leq 10$.
- The proposed model can give designers and engineers a scope for proper selection of material distribution, especially in manufacturing of nanosensors and nanoactuators.

Acknowledgments This work was funded by the Deanship of Scientific Research (DSR), King Abdulaziz University, Jeddah, under Grant No. (135-790-D1435). The authors, therefore, acknowledge DSR technical and financial support.

References

1. M.A. Agwa, M.A. Eltaher, Vibration of a carbyne nanomechanical mass sensor with surface effect. Appl. Phys. A **122**(4), 1–8 (2016)
2. M. Ahouel, M.S.A. Houari, E.A. Bedia, A. Tounsi, Size-dependent mechanical behavior of functionally graded trigonometric shear deformable nanobeams including neutral surface position concept. Steel Compos. Struct. **20**(5), 963–981 (2016)
3. A.E. Alshorbagy, M.A. Eltaher, F.F. Mahmoud, Free vibration characteristics of a functionally graded beam by finite element method. Appl. Math. Model. **35**(1), 412–425 (2011)
4. H.A. Atmane, A. Tounsi, S.A. Meftah, H.A. Belhadj, Free vibration behavior of exponential functionally graded beams with varying cross-section. J. Vib. Control **17**(2), 311–318 (2010)
5. Z. Belabed, M.S.A. Houari, A. Tounsi, S.R. Mahmoud, O.A. Bég, An efficient and simple higher order shear and normal deformation theory for functionally graded material (FGM) plates. Compos. Part B Eng. **60**, 274–283 (2014)
6. H. Bellifa, K.H. Benrahou, L. Hadji, M.S.A. Houari, A. Tounsi, Bending and free vibration analysis of functionally graded plates using a simple shear deformation theory and the concept the neutral surface position. J. Braz. Soc. Mech. Sci. Eng. **38**(1), 265–275 (2016)
7. S. Benguediab, A. Tounsi, M. Zidour, A. Semmah, Chirality and scale effects on mechanical buckling properties of zigzag double-walled carbon nanotubes. Compos. Part B Eng. **57**, 21–24 (2014)
8. M. Bennoun, M.S.A. Houari, A. Tounsi, A novel five-variable refined plate theory for vibration analysis of functionally graded sandwich plates. Mech. Adv. Mater. Struct. **23**(4), 423–431 (2016)
9. S. Ben-Oumrane, T. Abedlouahed, M. Ismail, B.B. Mohamed, M. Mustapha, A.B. El Abbas, A theoretical analysis of flexional bending of Al/Al 2 O 3 S-FGM thick beams. Comput. Mater. Sci. **44**(4), 1344–1350 (2009)
10. A. Besseghier, H. Heireche, A.A. Bousahla, A. Tounsi, A. Benzair, Nonlinear vibration properties of a zigzag single-walled carbon nanotube embedded in a polymer matrix. Adv. Nano Res. **3**(1), 29–37 (2015)
11. F. Bounouara, K.H. Benrahou, I. Belkorissat, A. Tounsi, A nonlocal zeroth-order shear deformation theory for free vibration of functionally graded nanoscale plates resting on elastic foundation. Steel Compos. Struct. **20**(2), 227–249 (2016)
12. B. Bouderba, M.S.A. Houari, A. Tounsi, Thermomechanical bending response of FGM thick plates resting on Winkler–Pasternak elastic foundations. Steel Compos. Struct. **14**(1), 85–104 (2013)
13. M. Bourada, A. Kaci, M.S.A. Houari, A. Tounsi, A new simple shear and normal deformations theory for functionally graded beams. Steel Compos. Struct. **18**(2), 409–423 (2015)
14. F.L. Chaht, A. Kaci, M.S.A. Houari, A. Tounsi, O.A. Beg, S.R. Mahmoud, Bending and buckling analyses of functionally graded material (FGM) size-dependent nanoscale beams including the thickness stretching effect. Steel Compos. Struct. **18**(2), 425–442 (2015)
15. S.H. Chi, Y.L. Chung, Cracking in sigmoid functionally graded coating. J. Mech. **18**, 41–53 (2002)
16. F. Delale, F. Erdogan, The crack problem for a nonhomogeneous plane. J. Appl. Mech. **50**(3), 609–614 (1983)
17. N.D. Duc, P.H. Cong, Nonlinear dynamic response of imperfect symmetric thin sigmoid-functionally graded material plate with metal–ceramic–metal layers on elastic foundation. J. Vib. Control **21**, 637–646 (2013)
18. F. Ebrahimi, E. Salari, Size-dependent free flexural vibrational behavior of functionally graded nanobeams using semi-analytical differential transform method. Compos. Part B Eng. **79**, 156–169 (2015)
19. F. Ebrahimi, M. Boreiry, Investigating various surface effects on nonlocal vibrational behavior of nanobeams. Appl. Phys. A **121**(3), 1305–1316 (2015)
20. F. Ebrahimi, M.R. Barati, Dynamic modeling of a thermo–piezo-electrically actuated nanosize beam subjected to a magnetic field. Appl. Phys. A **122**(4), 1–18 (2016)
21. M.A. Eltaher, S.A. Emam, F.F. Mahmoud, Free vibration analysis of functionally graded size-dependent nanobeams. Appl. Math. Comput. **218**(14), 7406–7420 (2012)

22. M.A. Eltaher, S.A. Emam, F.F. Mahmoud, Static and stability analysis of nonlocal functionally graded nanobeams. Compos. Struct. **96**, 82–88 (2013)
23. M.A. Eltaher, A.E. Alshorbagy, F.F. Mahmoud, Determination of neutral axis position and its effect on natural frequencies of functionally graded macro/nanobeams. Compos. Struct. **99**, 193–201 (2013)
24. M.A. Eltaher, A.E. Alshorbagy, F.F. Mahmoud, Vibration analysis of Euler-Bernoulli nanobeams by using finite element method. Appl. Math. Model. **37**(7), 4787–4797 (2013)
25. M.A. Eltaher, A. Khairy, A.M. Sadoun, F.A. Omar, Static and buckling analysis of functionally graded Timoshenko nanobeams. Appl. Math. Comput. **229**, 283–295 (2014)
26. M.A. Eltaher, A.A. Abdelrahman, A. Al-Nabawy, M. Khater, A. Mansour, Vibration of nonlinear graduation of nano-Timoshenko beam considering the neutral axis position. Appl. Math. Comput. **235**, 512–529 (2014)
27. M.A. Eltaher, M.E. Khater, S.A. Emam, A review on nonlocal elastic models for bending, buckling, vibrations, and wave propagation of nanoscale beams. Appl. Math. Model. **40**(5–6), 4109–4128 (2016)
28. M.A. Eltaher, S. El-Borgi, J.N. Reddy, Nonlinear analysis of size-dependent and material-dependent nonlocal CNTs. Compos. Struct. **153**, 902–913 (2016)
29. A.C. Eringen, Nonlocal polar elastic continua. Int. J. Eng. Sci. **10**(1), 1–16 (1972)
30. A.C. Eringen, D.G.B. Edelen, On nonlocal elasticity. Int. J. Eng. Sci. **10**(3), 233–248 (1972)
31. A.C. Eringen, On differential equations of nonlocal elasticity and solutions of screw dislocation and surface waves. J. Appl. Phys. **54**(9), 4703–4710 (1983)
32. A. Fereidoon, A. Mohyeddin, Bending analysis of thin functionally graded plates using generalized differential quadrature method. Arch. Appl. Mech. **81**(11), 1523–1539 (2011)
33. S. Filiz, M. Aydogdu, Wave propagation analysis of embedded (coupled) functionally graded nanotubes conveying fluid. Compos. Struct. **132**, 1260–1273 (2015)
34. A. Hamidi, M.S.A. Houari, S.R. Mahmoud, A. Tounsi, A sinusoidal plate theory with 5-unknowns and stretching effect for thermomechanical bending of functionally graded sandwich plates. Steel Compos. Struct. **18**(1), 235–253 (2015)
35. H. Hebali, A. Tounsi, M.S.A. Houari, A. Bessaim, E.A.A. Bedia, New quasi-3D hyperbolic shear deformation theory for the static and free vibration analysis of functionally graded plates. J. Eng. Mech. **140**(2), 374–383 (2014)
36. S.A.H. Hosseini, O. Rahmani, Free vibration of shallow and deep curved FG nanobeam via nonlocal Timoshenko curved beam model. Appl. Phys. A **122**(3), 1–11 (2016)
37. W.Y. Jung, S.C. Han, Analysis of sigmoid functionally graded material (S-FGM) nanoscale plates using the nonlocal elasticity theory. Math. Problems Eng. **49**, 449–458 (2013)
38. S. Kapuria, M. Bhattacharyya, A.N. Kumar, Bending and free vibration response of layered functionally graded beams: a theoretical model and its experimental validation. Compos. Struct. **82**(3), 390–402 (2008)
39. K. Kiani, Longitudinal and transverse instabilities of moving nanoscale beam-like structures made of functionally graded materials. Compos. Struct. **107**, 610–619 (2014)
40. M. Komijani, S.E. Esfahani, J.N. Reddy, Y.P. Liu, M.R. Eslami, Nonlinear thermal stability and vibration of pre/post-buckled temperature-and microstructure dependent functionally graded beams resting on elastic foundation. Compos. Struct. **112**, 292–307 (2014)
41. C.Y. Lee, J.H. Kim, Thermal post-buckling and snap-through instabilities of FGM panels in hypersonic flows. Aerosp. Sci. Technol. **30**(1), 175–182 (2013)
42. S.R. Li, H.D. Su, C.J. Cheng, Free vibration of functionally graded material beams with surface-bonded piezoelectric layers in thermal environment. Appl. Math. Mech. **30**, 969–982 (2009)
43. X.F. Li, Y.A. Kang, J.X. Wu, Exact frequency equations of free vibration of exponentially functionally graded beams. Appl. Acoust. **74**(3), 413–420 (2013)
44. Y. Liu, D.W. Shu, Free vibration analysis of exponential functionally graded beams with a single delamination. Compos. Part B Eng. **59**, 166–172 (2014)
45. A. Mahi, E.A. Bedia, A. Tounsi, I. Mechab, An analytical method for temperature-dependent free vibration analysis of functionally graded beams with general boundary conditions. Compos. Struct. **92**(8), 1877–1887 (2010)
46. A. Mahi, A. Tounsi, A new hyperbolic shear deformation theory for bending and free vibration analysis of isotropic, functionally graded, sandwich and laminated composite plates. Appl. Math. Model. **39**(9), 2489–2508 (2015)
47. M.A.A. Meziane, H.H. Abdelaziz, A. Tounsi, An efficient and simple refined theory for buckling and free vibration of exponentially graded sandwich plates under various boundary conditions. J. Sandw. Struct. Mater. **16**(3), 293–318 (2014)
48. T. Mori, K. Tanaka, Average stress in matrix and average elastic energy of materials with misfitting inclusions. Acta Metall. **21**(5), 571–574 (1973)
49. O. Rahmani, A.A. Jandaghian, Buckling analysis of functionally graded nanobeams based on a nonlocal third-order shear deformation theory. Appl. Phys. A **119**(3), 1019–1032 (2015)
50. O. Rahmani, O. Pedram, Analysis and modeling the size effect on vibration of functionally graded nanobeams based on nonlocal Timoshenko beam theory. Int. J. Eng. Sci. **77**, 55–70 (2014)
51. J.N. Reddy, Nonlocal theories for bending, buckling and vibration of beams. Int. J. Eng. Sci. **45**(2), 288–307 (2007)
52. J.N. Reddy, S. El-Borgi, Eringen's nonlocal theories of beams accounting for moderate rotations. Int. J. Eng. Sci. **82**, 159–177 (2014)
53. J.N. Reddy, S. El-Borgi, J. Romanoff, Non-linear analysis of functionally graded microbeams using Eringen's non-local differential model. Int. J. Non-Linear Mech. **67**, 308–318 (2014)
54. H. Salehipour, A.R. Shahidi, H. Nahvi, Modified nonlocal elasticity theory for functionally graded materials. Int. J. Eng. Sci. **90**, 44–57 (2015)
55. M. Şimşek, H.H. Yurtcu, Analytical solutions for bending and buckling of functionally graded nanobeams based on the nonlocal Timoshenko beam theory. Compos. Struct. **97**, 378–386 (2013)
56. R. Sourki, S.A.H. Hoseini, Free vibration analysis of size-dependent cracked microbeam based on the modified couple stress theory. Appl. Phys. A **122**(4), 1–11 (2016)
57. T.R. Tauchert, *Energy Principles in Structural Mechanics* (McGraw-Hill Companies, New York, 1974)
58. Y. Tomota, K. Kuroki, T. Mori, I. Tamura, Tensile deformation of two-ductile phase alloys: flow curves of α–γ Fe–Cr–Ni alloys. Mater. Sci. Eng. **24**(1), 85–94 (1976)
59. A. Tounsi, S. Benguediab, B. Adda, A. Semmah, M. Zidour, Nonlocal effects on thermal buckling properties of double-walled carbon nanotubes. Adv. Nano Res. **1**(1), 1–11 (2013)
60. B. Uymaz, Forced vibration analysis of functionally graded beams using nonlocal elasticity. Compos. Struct. **105**, 227–239 (2013)
61. S.A. Yahia, H.A. Atmane, M.S.A. Houari, A. Tounsi, Wave propagation in functionally graded plates with porosities using various higher-order shear deformation plate theories. Struct. Eng. Mech. **53**(6), 1143–1165 (2015)
62. M. Zidi, A. Tounsi, M.S.A. Houari, O.A. Bég, Bending analysis of FGM plates under hygro-thermo-mechanical loading using a four variable refined plate theory. Aerosp. Sci. Technol. **34**, 24–34 (2014)